

Modeling of a standalone Wind-PV Hybrid generation system using MATLAB/SIMULINK and its performance analysis

Mohammed Aslam Husain, Abu Tariq

Abstract—This work focuses on the modeling and analysis of a Standalone wind-PV Hybrid generation system under different conditions in MATLAB/SIMULINK environment. The proposed system consists of two renewable sources i.e. wind and solar energy. Modeling of PV array and wind turbine is clearly explained. The wind subsystem is equipped of a direct driven permanent-magnet synchronous generator, a diode rectifier and a buck converter for the tracking of the maximum power point. In photovoltaic system the variable DC output voltage is controlled by another buck converter used for the MPPT. These two systems are combined to operate in parallel and the common DC bus collects the total energy from the wind and photovoltaic subsystems and uses it partly to charge the battery and partly to the DC load. This paper offers a useful wind-PV hybrid model which can be used for performance analysis of such systems.

Index Terms—Buck converter , Insolation, MATLAB simulation , PV array, PMSG , temperature, turbine, wind speed.

1 INTRODUCTION

THE rising consumption rate of fossil fuels and the pollution problem associated with them has drawn worldwide attention towards renewable energy sources. A combination of two or more renewable energy sources is more effective as compared to single source system in terms of cost, efficiency and reliability. Properly chosen renewable power sources will considerably reduce the need for fossil fuel leading to an increase in the sustainability of the power supply. Standalone Wind/PV hybrid generation system offers a feasible solution to distributed power generation for isolated localities where utility grids are not available. It is also free from pollution what makes it more attractive. For isolated localities, one practical approach to self-sufficient power generation involves using a wind turbine and PV system with battery storage to create a stand-alone hybrid system [1, 2]. The common types of AC generator in modern wind turbine systems are as follows: Squirrel-Cage rotor Induction Generator; Wound-Rotor Induction Generator; Doubly-Fed Induction Generator; Synchronous Generator (With external field excitation); and Permanent Magnet Synchronous Generator [3]. However, in this paper the variable-speed directly-driven multi-pole permanent magnet synchronous generator (PMSG) wind architecture is chosen for this purpose, it offers better performance due to higher efficiency and less maintenance because it does not have rotor current. PMSG can be used without a gearbox, which implies a reduction of the weight of the nacelle and reduction of costs [1].

A photovoltaic (PV) system is the most simple and reliable way to produce electricity from the conversion of solar energy. The basic building device of SPV system is SPV cell. The output of SPV system may be directly fed to the loads or may use a power electronic converter to operate it at its maximum power point. [5,6].

The main task of this paper is to develop a simulation model of a standalone hybrid generation System including wind and PV subsystems using MATLAB/SIMULINK system. Characteristics of modeled wind turbine and PV panel have been shown for different conditions. This paper includes in details the equations that form the wind turbine and PV panel. The two systems are combined to operate in parallel. Each of the two subsystems; namely PV subsystem and wind subsystem is controlled by its own controller. Each controller will guide its own system to track the maximum power [4, 5]. The aim of this paper is to provide the reader with all necessary information to develop wind turbine models and PV panel that can be used in the simulation for a standalone wind/PV generation system and for further study of such systems.

2 MODELING OF WIND TURBINE

The power captured from the wind turbine is given as by relation [1,2]. ρ is the air density, which is equal to 1.225 kg/m³, C_p is the power coefficient V_w is the wind speed in m/s and A is the area swept by the rotor in m².

$$P_w = 1/2 C_p \rho A V_w^3 \quad (1)$$

The amount of aerodynamic torque T_w in N-m is given by the ratio between the power extracted from the wind and the turbine rotor speed w_w in rad/s, as follows

$$T_w = P_w / w_w \quad (2)$$

Mechanical torque transmitted to the generator is the same as the aerodynamic torque since there is no gearbox. The power coefficient C_p reaches maximum value equal to 0.593 which means that the power extracted from the wind is always less than 59.3% (Betz's limit) because various aerodynamic losses

- Mohammed Aslam Husain is currently working as Assistant Professor in Department of Electrical Engineering, Aligarh Muslim University, ZHCET, Aligarh, INDIA. E-mail: mahusain87@gmail.com
- Dr. Abu Tariq is currently working as Associate Professor in Department of Electrical Engineering, Aligarh Muslim University, ZHCET, Aligarh, INDIA. E-mail: mahusain87@gmail.com

depend on rotor construction [6, 7]. The general function defining the power coefficient as a function of the tip speed ratio

$$C_p(\lambda, \vartheta) = c_1(c_2 \frac{1}{\beta} - c_3 \vartheta - c_4 \vartheta^x - c_5) e^{-c_5/\beta}$$

and the blade pitch angle is defined as

Since this function depends on the wind turbine rotor type, the coefficient c_1 - c_6 and x can be different for various turbines. The coefficients are equal to: $c_1=0.5, c_2=116, c_3=0.4, c_4=0, c_5=5, c_6=21$ (x is not used because $c_4=0$). Additionally the parameter is also defined as

$$\frac{1}{\beta} = \frac{1}{\lambda + 0.08\theta} - \frac{0.035}{1 + \theta^3} \quad (4)$$

Where θ is the pitch angle and the tip speed ratio λ is defined as

$$\lambda = \omega_w R / V_w \quad (5)$$

Where ω_w is the angular velocity of rotor [rad/s], R is the rotor radius [m] and V_w is wind speed [m/s] [1, 2, 8].

The model of the wind turbine implemented in Simulink is shown in figure 1 and figure 2 shows the mask of wind turbine [4,6].

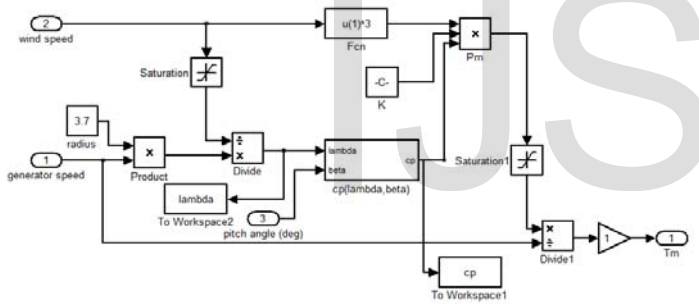


Fig. 1. Wind Turbine model

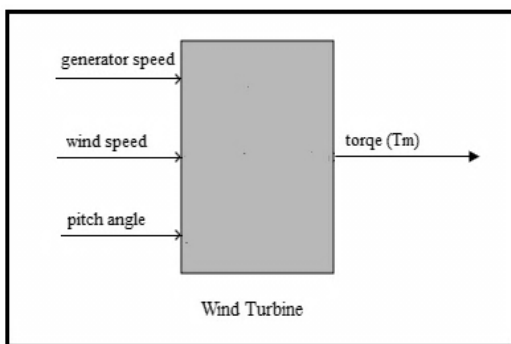


Fig. 2. Mask of Wind Turbine

3 PMSG WIND ENERGY GENERATION SYSTEM

The direct driven wind turbine concept with multi-pole permanent magnet synchronous generator (PMSG) and full-scale frequency converter is an auspicious but not yet very popular wind turbine concept for modern wind turbines[8].

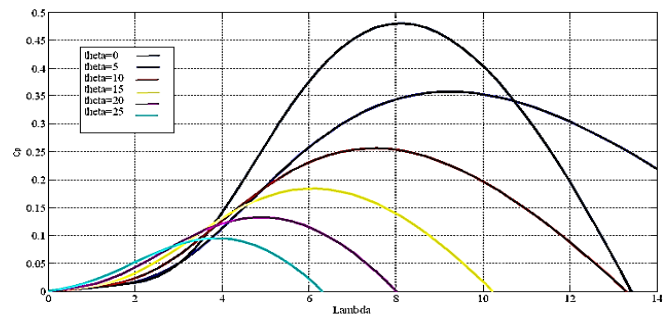


Fig. 3. Cp vs. Lambda characteristics for various blade pitch angle

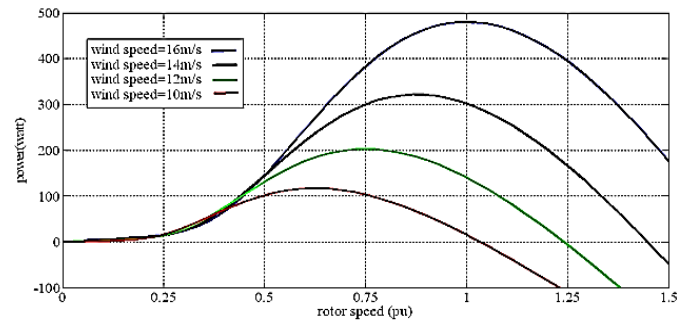


Fig. 4. Power vs. speed curves for different wind speeds

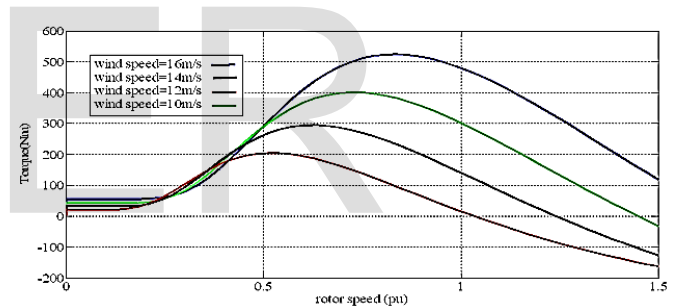


Fig. 5. Torque vs. speed curves for different wind speeds.

Since a gearbox causes higher weight, losses, costs and demands maintenance, a gearless construction represents an efficient and robust solution, which could be very beneficial especially for offshore applications. Moreover, due to the permanent magnet excitation of the generator the DC excitation system can be eliminated reducing again weight, losses, costs and maintenance requirements. The efficiency of a PMSG wind turbine is thus assessed to be higher than for other concepts. However, the disadvantages of the permanent magnet excitation are the still high costs for permanent magnet materials and a fixed excitation, which cannot be changed according to the operational point. As multi-pole permanent magnet generators are low speed applications and generally connected to the grid through a frequency converter system, the generator has no damper winding in the rotor core. Moreover, due to the permanent excitation a PMSG has no field windings, in which transient currents could be induced or damped respectively. Hence, in case of load changes the field windings would not contribute to damping either. As neither a damper nor field-winding exists in a PMSG, no transient or sub-transient reac-

tances, as known for wound rotor SGs, can be defined for the PMSG.

i.e.
 $X_d = X_d' = X_d''$
 $X_q = X_q' = X_q''$

X_d and X_q - synchronous reactance
 X_d' and X_q' - transient reactance
 X_d'' and X_q'' - sub-transient reactance

However, as the multi-pole PMSG is a low speed application with slow dynamics, a damper winding is less important. However, a damping of the system must then be applied by means of the converter control [7, 8].

DC-DC converter is used to buck the rectified voltage. In the converter circuit the gate receives the pulse from PWM generator. The corresponding Simulink model is shown in Figure 7. A 480W, 34 pole, 300 rpm rated speed, permanent-magnet synchronous generator (PMSG), a diode rectifier and a (DC/DC) buck converter for the tracking of the maximum power point is used in this model. Lead acid battery used here has a nominal voltage rating of 48V [4, 5].

4 MODELING OF PHOTOVOLTAIC CELL

The basic equation from the theory of semiconductors [9] that mathematically describes the I-V characteristic of the ideal photovoltaic cell is:

$$I_C = I_{ph} - I_0 \left(e^{\frac{qV_C}{kT_C}} - 1 \right) \quad (6)$$

Where: I_{ph} is the short-circuit current that is equal to the photon generated current.

$$I_d = I_0 \left(e^{\frac{qV_d}{kT_c}} - 1 \right) \quad (7)$$

I_d is the current shunted through the intrinsic diode. The diode current I_d is given by the Shockley's diode equation; V_d is the voltage across the diode (D). k is Boltzmann constant, q is electron charge, I_0 is reverse saturation current of diode, T_c is reference cell operating temperature (25 °C). Practical arrays are composed of several connected photovoltaic cells and the observation of the characteristics at the terminals of the photovoltaic array requires the inclusion of additional parameters to basic equation [9, 13, 14].

Figure 6 shows Single-diode model of the theoretical photovoltaic cell and Fig.7 shows the I-V curve for a solar cell for different load. If the load R is small, the cell operates in the region M-N of Fig.7, where the cell behaves as a constant current source, almost equal to the short circuit current. On the other hand, if the load R is large, the cell operates on the regions P-S of the curve, the cell behaves more as a constant voltage source, almost equal to the open-circuit voltage [11, 12]. Equation 8 represents the practical SPV cell equation and describes the single-diode model presented in Fig.6. I_{ph} is the saturation current of the array. $V_t = N_s k T / q$ is the thermal voltage of the array with N_s cells connected in series. R_s is the equivalent series resistance of the array and R_p is the equivalent parallel resistance.

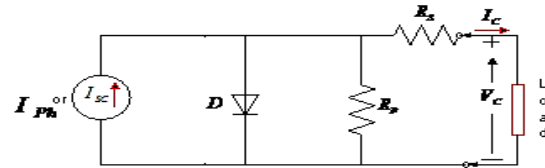


Fig.6: Single-diode model of the theoretical photovoltaic cell.

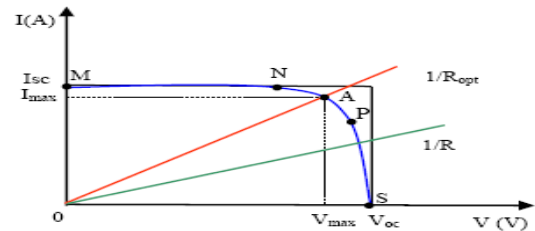


Fig.7: A typical, current-voltage I-V curve for a solar cell for different load.

$$I_C = I_{ph} - I_0 \left[e^{\frac{q(V_C + I_C R_s)}{A k T_c}} - 1 \right] - \left(\frac{V_C + I_C R_s}{R_p} \right) \quad (8)$$

Figure 7 is obtained using Equation 3 [9, 10].

$$I_{pv} = (I_{pv,n} + K_1 \Delta T) G / G_n \quad (9)$$

Where $I_{pv,n}$ [A] is the light-generated current at the nominal condition (usually 25 °C and 1000W/m²), $\Delta T = T - T_n$, G [W/m²] is the irradiation on the device surface, and G_n is the nominal irradiation.

$$I_0 = \frac{I_{sc,n} + K_1 \Delta T}{\exp\left(\frac{V_{oc,n} + K_2 \Delta T}{a V_t}\right) - 1} \quad (10)$$

The reverse saturation current at the reference temperature is given by the eq. 10 [9, 10, 15]. The value of the diode constant 'a' may be arbitrarily chosen. Many authors discuss ways to estimate the correct value of this constant. Usually $1 \leq a \leq 1.5$ [10]. Equation 11 shows the PV cell model current, I_m , referring to the appropriate model circuit as in figure 6 [9].

$$I = I_{pv} - I_0 \left[\exp\left(\frac{V + R_s I}{a V_t}\right) - 1 \right] \quad (11)$$

Equation 12 depicts the equation used to model PV array.

$$I_m = (N_{pp} * I_{pv}) - (N_{pp} * I_0) \left[\exp\left(\frac{V / N_{ss} + R_{sl} / N_{pp}}{a V_t}\right) - 1 \right] \quad (12)$$

Table I shows the parameters of the PV module. The simulation results of the PV module are shown in Fig.8 & Fig.9.

Table I. Parameters used in PV module for the different characteristics

S.No	Parameters	Value
1	V_{oc}	85V
2	I_{sc}	5.68A
3	K_i	0.0032A/K
4	K_v	-0.1230V/K
5	N_s	54
6	R_s	0.221Ω

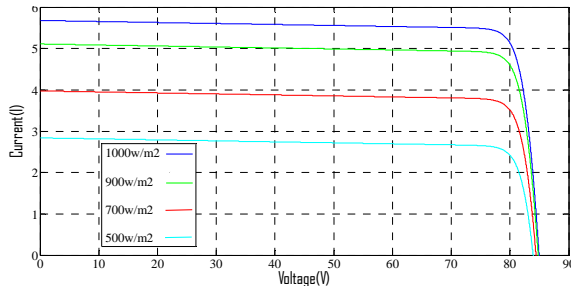


Fig. 8: $i-v$ characteristics of solar array at variable solar insolation, 25°C

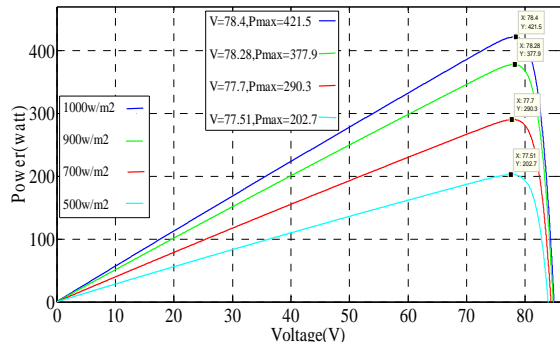


Fig. 9: $p-v$ characteristics at variable temperature, $1000\text{W}/\text{m}^2$

5 WIND-PV HYBRID GENERATION SYSTEM

Figure 10 shows the proposed system which consists of a wind turbine, a variable speed direct-drive wind generator, a wind-side ac/dc converter, a solar array, dc/dc converters and a common dc load in parallel with a battery.

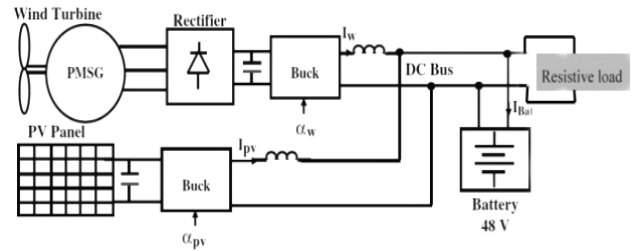


Fig. 10: Standalone wind/PV hybrid system
 Mechanical energy from the wind turbine drives the wind generator to generate a.c. electric power, which is converted into d.c. power to form the common dc link. PV array generates dc power [4, 5]. Each of the two subsystems; namely PV subsystem and wind subsystem is controlled by its own controller. Each controller will guide its own system to track the maximum power [4, 5, 16]. The system power output depends on the climatic conditions (wind, sun), and on the battery state of charge. It can be tested for different system operations.

The control strategy used here controls the battery state of charge by keeping the DC bus voltage around the rated battery voltage (i.e.48V).The wind subsystem is a 480 W wind generator equipped of a direct driven permanent-magnet synchronous generator (PMSG), a diode rectifier and a (DC/DC) buck converter for the tracking of the maximum power point.

A 420 W photovoltaic panel is used, whose variable DC output voltage is controlled by another (DC/DC) buck used for the MPPT. The common DC bus collects the total energy from the wind and photovoltaic subsystems and uses it partly to charge the battery and partly to the DC load. Figure 11 shows the block diagram of simulated standalone hybrid PV-Wind system.

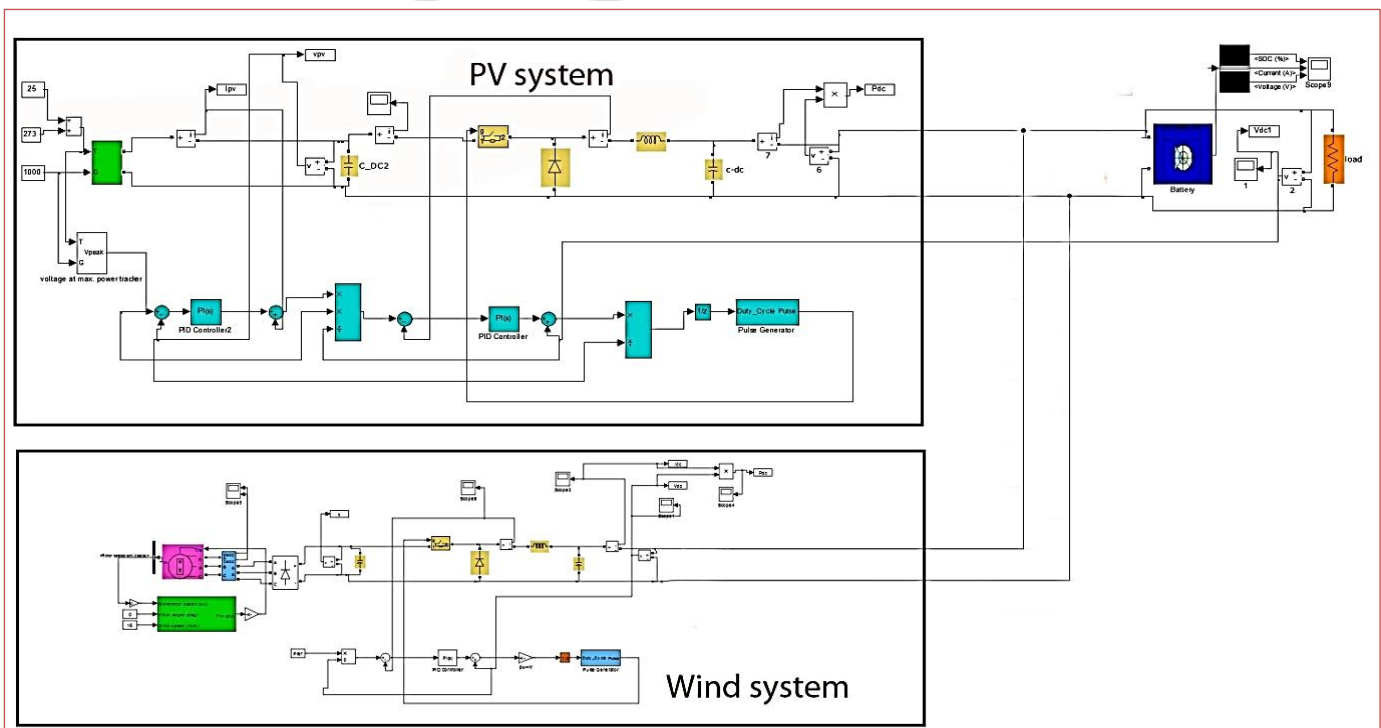


Fig. 11: Block diagram of standalone hybrid system

6 SIMULATION RESULTS

In figures 12 and 13 at time t_1 the power output of PV system reaches its maximum steady state value of 421.5watts at $1000w/m^2$. At t_3 the insolation starts decreasing linearly till t_7 and reaches $500w/m^2$, so the power output of PV system also decreases linearly and reaches a value of 202.7watts. At t_2 the power output of wind system reaches its maximum value of 479.8watts at 16m/s. As the wind speed changes to 14m/s at t_5 , the power output of wind system changes to 321.5 watts.

Figure 13 shows the variation of output current and voltage of the hybrid system. The power output of hybrid system shown by red line in figure 14 is almost equal to the sum of power outputs of both wind and PV system at any instant of time. At t_2 power output of hybrid system is almost equal to 900watts which is equal to the sum of power output of wind (479watts) and PV (421watts) system at t_2 .

Figures 14, 15 and 16 show and explain different characteristics of the Hybrid system for step change in wind speed from 16 to 14m/s and for linear change in insolation from 1000 to $500w/m^2$ and back to $1000w/m^2$.

Similarly figures 17, 18 and 19 show and explain different characteristics of the Hybrid system for step change in wind speed from 16 to 14m/s and for a step change in temperature from 25 to $40^\circ C$. With change in insolation, temperature and wind speed the output power of the standalone hybrid system changes and power sharing between PV and wind system is shown in table II.

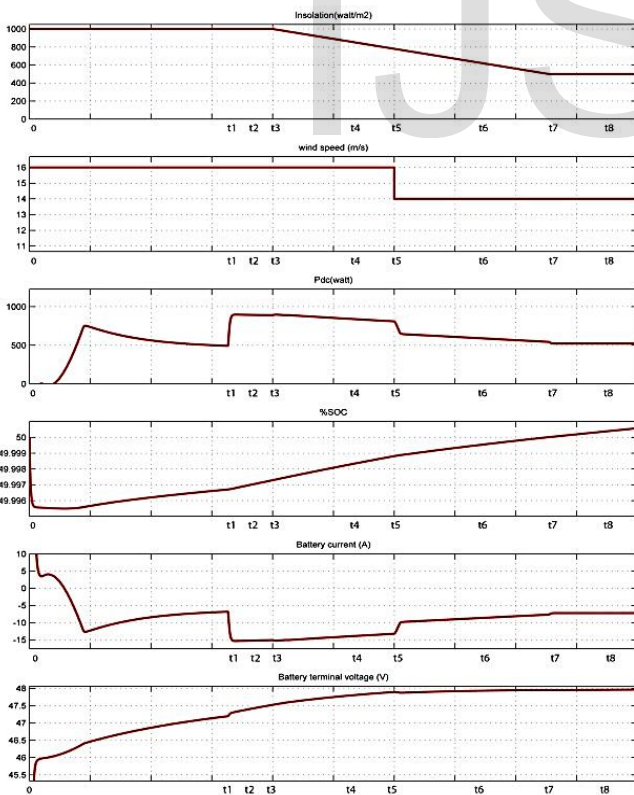


Fig. 12: Different characteristics of the Hybrid system for step change in wind speed from 16 to 14m/s and for a linear change in insolation from 1000 to $500w/m^2$.

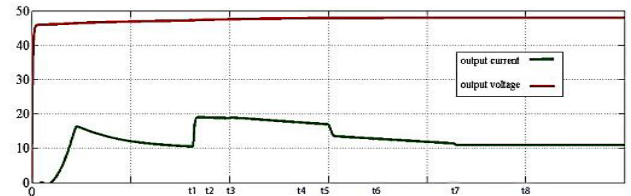


Fig.13: Output voltage and current of Hybrid system for step change in wind speed from 16 to 14m/s and for a linear change in insolation from

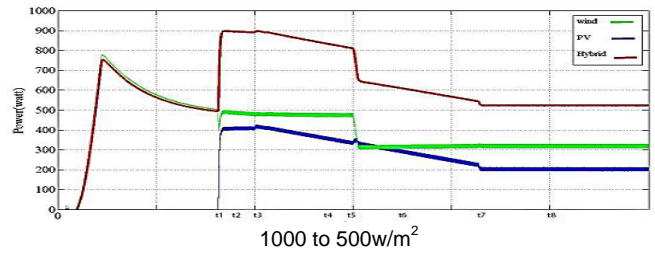


Fig. 14: Power output of different systems for step change in wind speed from 16 to 14m/s and for a linear change in insolation from 1000 to

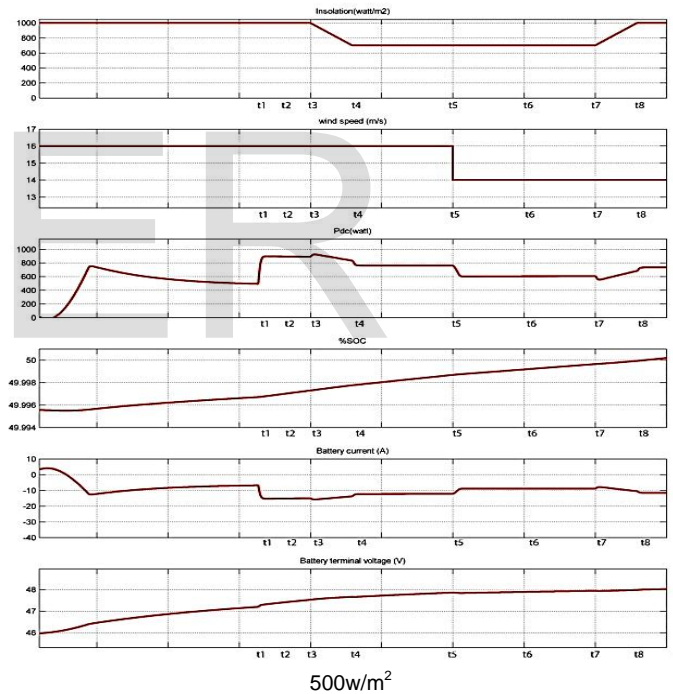


Fig. 15: Different characteristics of the Hybrid system for step change in wind speed from 16 to 14m/s and for linear change in insolation from 1000

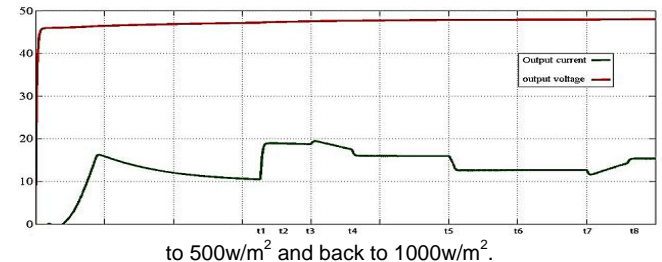


Fig. 16: Output voltage and current of Hybrid system for step change in wind speed from 16 to 14m/s and for linear change in insolation from 1000 to $500w/m^2$ and back to $1000w/m^2$.

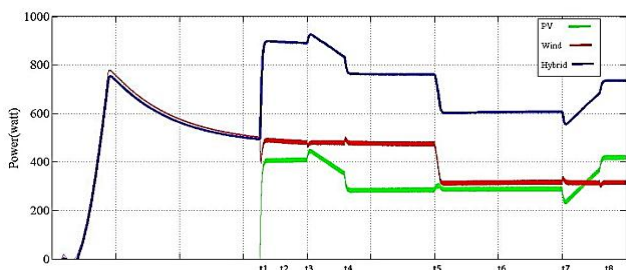


Fig.17: Power output of different systems for step change in wind speed from 16 to 14m/s and for linear change in insolation from 1000 to 500w/m² and back to 1000w/m².

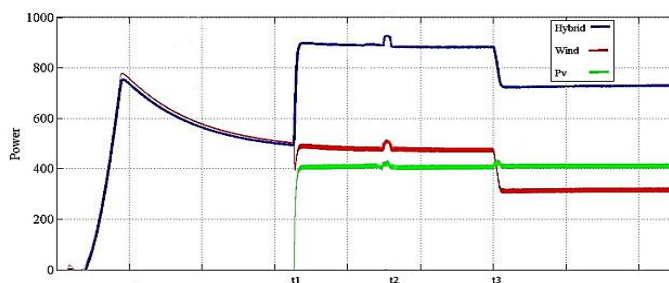


Fig.20: Power output of different systems for step change in wind speed from 16 to 14m/s and for a step change in temperature from 25 to 40°C.

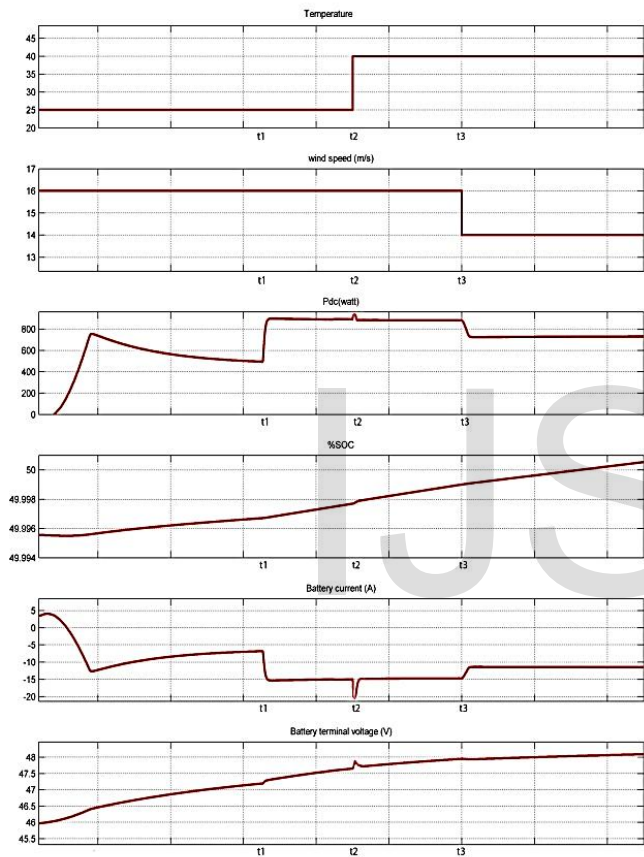


Fig.18: Different characteristics of the Hybrid system for step change in wind speed from 16 to 14m/s and for a step change in temperature from 25 to 40°C.

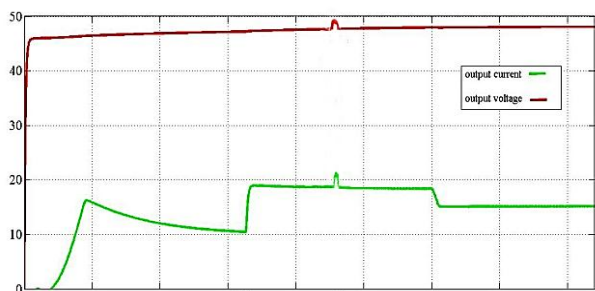


Fig. 19: Output voltage and current of Hybrid system for step change in wind speed from 16 to 14m/s and for a step change in temperature from 25 to 40°C.

TABLE II. POWER OUTPUT OF STANDALONE HYBRID SYSTEM FOR DIFFERENT CONDITIONS

Insolation (W/m ²)	Temp. (°C)	Wind speed(m/s)	Output Power(W)		
			PV sharing system	Wind system sharing	Hybrid system
1000	25	16	420.9	479.2	900.1
500	25	14	202	320.7	522.7
1000	40	16	418.5	479.3	897.8

7 CONCLUSION

Feasibility study of a Wind-PV hybrid generation system was conducted at designing stage. ASIMULINK model of the Wind-PV hybrid generation system is proposed and all the necessary models of the system components were addressed. Various results were obtained at different operating conditions and these results were found to be satisfactory. Power sharing by each subsystem was also found to be in accordance. This paper is very useful for modelling and for basic analysis of Wind-PV hybrid system. With further modification this model can be used for the modelling of Grid connected Wind-PV system.

REFERENCES

- [1] Alejandro Rolan, Alvaro Luna, Gerardo Vazquez, Daniel Aguilar, Gustavo Azevedo, "Modeling of a Variable Speed Wind Turbine with a Permanent Magnet Synchronous Generator". IEEE International Symposium on Industrial Electronics (ISIE 2009) Seoul Olympic Parktel, Seoul, Korea July 5-8, 2009.
- [2] Polinder H., de Haan S. W. H., Dubois M. R., Slootweg J., "Basic Operation Principles and Electrical Conversion Systems of Wind Turbines", NORPIE / 2004, Nordic Workshop on Power and Industrial Electronics, Paper 069, Trondheim, Norway, 14-16 June, 2004.
- [3] Mittal R., Sandhu K. S. and Jain D. K. "Low voltage ride-through (LVRT) of grid interfaced wind driven PMSG," ARPN Journal of Engineering and Applied Sciences., 2009, vol. 4, no. 5. Pp. 73-83.
- [4] Dali M., Belhadj, J., Roboam, X. and Blaquiere, J.M. "Control and energy management of a wind photovoltaic hybrid system", Proc. EPE Conference, 2-5 Sept. 2007, pp 1-10.

- [5] Dali M., Belhadj J., Roboam X., "Hybrid solar-wind system with battery storage operating in grid-connected and standalone mode: Control and energy management - Experimental investigation", *Energy* 35 (2010) 2587-2595.
- [6] Akhmatov V., "Variable-Speed Wind Turbines with Doubly-Fed Induction Generators Part III: Model with the Back-to-back Converters", *Wind Engineering*, Volume 27, No. 2, pp 79-91, 2003
- [7] Hansen A.D., Michalke G., "Modelling and control of variable speed multipole PMSG wind turbine", submitted to *Wind Energy*, 2007.
- [8] Hong-Woo Kima, Sung-Soo Kimb, Hee-Sang Koa, "Modeling and control of PMSG-based variable-speed wind turbine", *Electric Power Systems Research* 80 (2010) 46-52.
- [9] I. Altas, A.M.Sharaf, 2007 "A photovoltaic array (PVA) simulation model to use in Matlab Simulink GUI environment." *IEEE I-4244-0632 -03/07*.
- [10] Marcelo Gradella Villalva, Jonas Rafael Gazoli, Ernesto Ruppert Filho, "Modeling and circuit-based simulation of photovoltaic arrays", 10th Brazilian Power Electronics Conference (COBEP), 2009.
- [11] J. Hyvarinen and J. Karila. New analysis method for crystalline silicon cells. In *Proc. 3rd World Conference on Photovoltaic Energy Conversion*, v. 2, p. 1521-1524, 2003.
- [12] E. Koutroulis, K. Kalaitzakis, and V. Tzitzilouis. Development of a FPGA-based system for real-time simulation of photovoltaic modules. *Microelectronics Journal*, 2008.
- [13] Geoff Walker. Evaluating MPPT converter topologies using a matlab PV model. *Journal of Electrical & Electronics Engineering, Australia*, 21(1), 2001.
- [14] W. De Soto, S. A. Klein, and W. A. Beckman. Improvement and validation of a model for photovoltaic array performance. *Solar Energy*, 80(1):78-88, January 2006.
- [15] Glass.M.C., "Improved solar array power point model with SPICE realization," in *Proc. 31st Intersoc. Energy Convers. Eng. Conf. (IECEC)*, 1996, vol. 1, pp. 286-291.
- [16] Kuo.Y.C., Liang.T.J. and Chen.J.F., "Novel maximum-power-point tracking controller for photovoltaic energy conversion system," *IEEE Trans. Ind. Electron.*, 2001, vol. 48, no. 3, pp. 594-601. Conclusion

Authors



generation and power electronics.

Mohammed Aslam Husain was born in Gorakhpur, India, in 1987. He received the B.Tech and M.Tech degree in electrical engineering from Aligarh Muslim University, Aligarh, in 2010 and 2012, respectively. Currently he is a faculty member in Department of Electrical Engineering, Aligarh Muslim University, Aligarh. His research interests include renewable energy

Dr. Abu Tariq obtained B.Sc Engg. and M.Tech Degree from Aligarh Muslim University in 1988 and 1999 respectively. He completed his Ph.D. from Aligarh Muslim University in 2006. Currently he is an Associate Professor in Department of Electrical engineering, Aligarh Muslim University. His research area includes Power Electronics and its Application on Photovoltaic Systems and Drives.

